Precoding Techniques for Turbo Codes

Ronald Garzon Bohorquez, Charbel Abdel Nour, Catherine Douillard

Precoding Techniques for Turbo Codes

Ronald Garzón Bohórquez, Charbel Abdel Nour, and Catherine Douillard
TELECOM Bretagne (Institut MINES-TELECOM), CNRS UMR 6285 Lab-STICC
Brest, France
Email: {ronald.garzonbohorquez, charbel.abdelnour, catherine.douillard}@telecom-bretagne.eu

***Abstract*—Among the various techniques to improve performance of Turbo Codes (TCs), it was shown that the prefixing of a rate-1 accumulator to a turbo encoder can represent a suitable solution that does not alter its coding rate. In this paper, we study the application of this precoding technique to improve the performance of TCs in the context of the Long Term Evolution (LTE) standard. To efficiently select the best precoder parameters in terms of convergence, we propose a design tool based on the real exchange of extrinsic information between the constituent SISO decoders. We also introduce two new precoding structures and we present design criteria leading to good interleavers for Precoded TCs (PTCs). Significant asymptotic performance improvements can be achieved with the proposed schemes.**

I. Introduction

In order to improve the error rate performance of Turbo Codes (TCs) [1], several types of interleaved code concatenations, called turbo-like codes [2], have been studied in past years. Iterative Soft Input Soft Output (SISO) decoding is performed at the receiver side where an exchange of extrinsic information is initiated between constituent decoders [3]. In [4], Abbasfar *et al.* studied the precoding technique applied to Accumulate Repeat Accumulate (ARA) codes. It was shown that the iterative decoding performance of such codes can be improved by prefixing a rate-1 accumulator to the encoder structure. This allows the decoding threshold of ARA codes to be reduced without altering their code rate. This technique was recently applied to TCs by Tong *et al.* [5] resulting in a new type of turbo-like codes named Precoded Turbo Codes (PTCs).

The basic PTC encoder structure considered in our study is shown in Fig. 1. The precoder is prefixed and connected to the TC via the interleaving function Π_1. It is composed of a serial-to-parallel converter block, a rate-1 accumulator and a parallel-to-serial converter block. As introduced in [5], only ρK bits of the data frame $\mathbf{d}$ are encoded by the accumulator, ρ being the precoding ratio. This parameter introduces a degree of freedom for code optimization.

In this paper, we first study the application of this precoding technique to improve the performance of the 8-state TC of the Long Term Evolution (LTE) standard [6]. Then, new precoding structures are proposed allowing asymptotic or convergence TC performance improvements. The rest of the paper is organized as follows. In Section II, we present a modified form of EXtrinsic Information Transfer (EXIT) charts suitable for the design of PTCs. Then, in Section III, we propose and analyze two new precoding structures. Finally, we derive relevant interleaver design criteria for the considered coding structure in Section IV and we present a performance example in Section V.

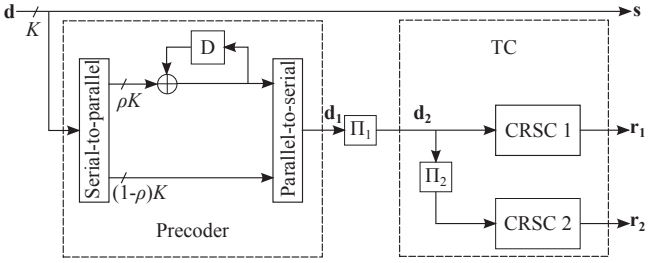

Fig. 1: Basic PTC encoder structure.

II. Modified EXIT chart analysis

As a first step, we carried out an analysis of the impact of the precoding ratio ρ on the convergence threshold of the reference precoding structure proposed in [5] and shown in Fig. 1, via conventional EXIT charts [7], [8]. The hierarchy convergence performance was not confirmed by the simulated error rate performance predicted by the EXIT charts. Consequently, these charts are *not* appropriate for the accurate determination of the best precoding ratio in terms of convergence.

In this section, we propose a modified EXIT chart scheme that is suitable for the selection of the precoding ratio value. Let us first identify the shortcomings of classic EXIT charts in the PTC context. One important parameter for EXIT charts is the distribution of the extrinsic Mutual Information (MI) at the input. Traditionally in the case of TCs where one SISO decoder receives *a priori* information from only one other SISO decoder, a Gaussian assumption is made. In the precoded case, *a priori* information on some of the bits (precoded ones) is available from the SISO decoder of the accumulator (SISO 0) *and* from the SISO decoder of CRSC 2 (SISO 2). Therefore, the distribution of the extrinsic mutual information at the input of one component SISO decoder is now different from the TC case. It can be even questioned if it follows a Gaussian distribution at all. In order to verify the validity of our reasoning, we have compared the distribution of the extrinsic information provided at the input of the SISO 1 decoder with the one generated via a Gaussian process, both having the same measured MI value. As shown in Fig. 2, for $\rho = 0.11$, $K = 1504$, and $R = 4/5$, the corresponding distributions are different. It proves that the extrinsic information samples at the input of SISO 1 cannot be generated from the same Gaussian process as in classic EXIT chart tools.

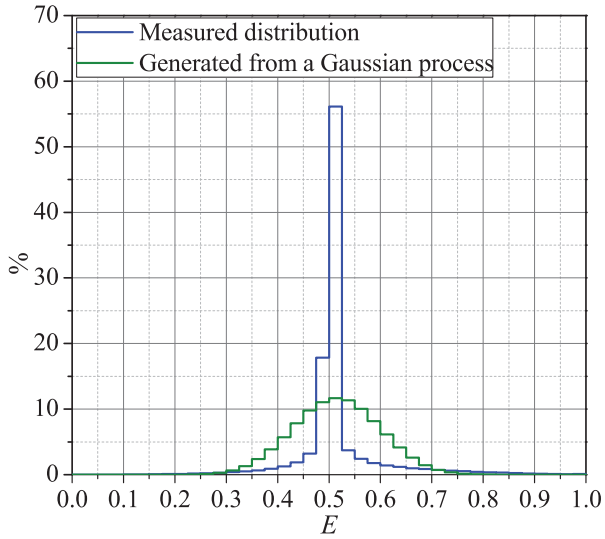

Fig. 2: Histograms of extrinsic information E at the input of SISO 1 generated in SISO 0 and SISO 2 without *a priori* information, for $\rho = 0.11$, $K = 1504$, and $R = 4/5$, evaluated at E_b/N_0 = 2 dB over the AWGN channel.

As a possible solution to this deviation, we propose to measure the *real* exchange of extrinsic information between the constituent SISO decoders of the TC, through the different PTC decoding iterations at the SNR value corresponding to the decoding threshold (see Fig. 3). In this modified EXIT chart, the best PTC parameters in terms of convergence performance are identified as those allowing a crossing point (IA, IE) as close as possible to (1, 1). The application of this modified EXIT chart to different precoding ratios is presented in Fig. 4, using uniform interleaving [9] for the 8-state CRSC$(13, 15)_8$ TC with coding rate $R = 4/5$, obtained by a periodic puncturing of parities, and data sequence size $K = 1504$. The simulated error rate curves of Fig. 5 validate this approach since the obtained convergence threshold hierarchy is the same as the one predicted in Fig. 4.

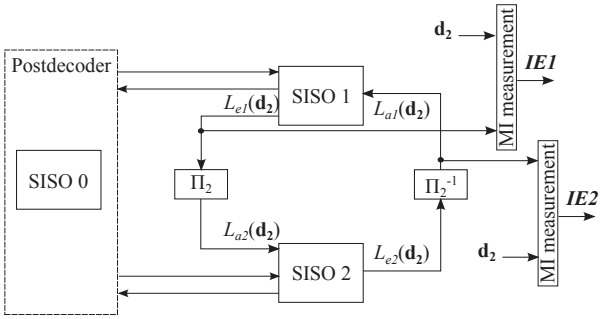

Fig. 3: Modified EXIT chart measurement.

III. Proposed Precoding Structures

In this section, two new precoding schemes are studied. The different precoding structures and parameters are compared

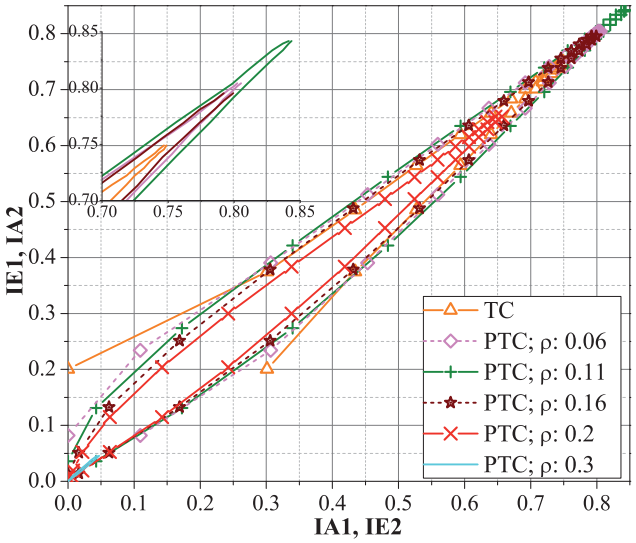

Fig. 4: Extrinsic information exchange between constituent codes of the TC at E_b/N_0 = 2.55 dB with 16 PTC decoding iterations, $K = 1504$, and $R = 4/5$ over the AWGN channel.

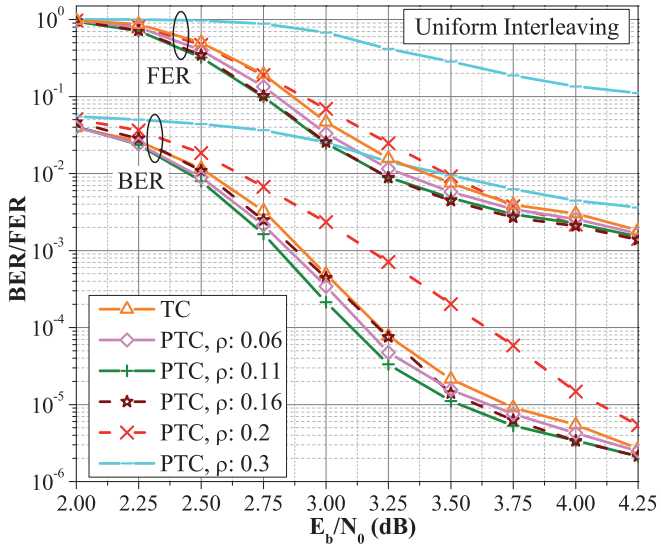

Fig. 5: PTC error rate performance for different values of ρ over the AWGN channel with BPSK modulation for $K = 1504$ and $R = 4/5$.

assuming uniform interleaving to average the interleavers effect on the error rate performance of the code.

A. Hybrid Precoding Structure

In the precoding structure of Fig. 1, ρK data symbols are encoded by the accumulator. Therefore, the extrinsic information exchange between the SISO decoder of the accumulator and the constituent SISO decoders of the TC is performed only on ρK turbo encoded bits. As an alternative to this PTC scheme, we propose a hybrid precoding structure, which precodes the whole data sequence and introduces a new parameter ϕ, $0 \leq \phi \leq 1$, to define the serial-to-parallel precoding ratio (see

Fig. 6(a)). Thus, ϕK parities and $(1-\phi)K$ data symbols of the accumulator are encoded by the TC. In the precoding mask, a precoder parity and a data position sent to the TC are identified by 1 and 0, respectively. The advantage of this precoding structure over the previous one is that it allows the SISO decoder of the accumulator to exchange extrinsic information on the whole turbo encoded sequence for all values of ϕ, as represented in Fig. 6(b). Note that for $\phi = 0$, the coding structure corresponds to the classic TC, since all the parities of the accumulator are punctured. By increasing the value of ϕ, the serial concatenation between the accumulator and the TC concerns a higher number of data bits. Therefore, asymptotic performance improvements are expected at the expense of a loss in convergence performance compared to the one of the classic TC. The tradeoff between convergence and asymptotic performance of the hybrid PTC is then controlled by the serial-to-parallel precoding ratio ϕ.

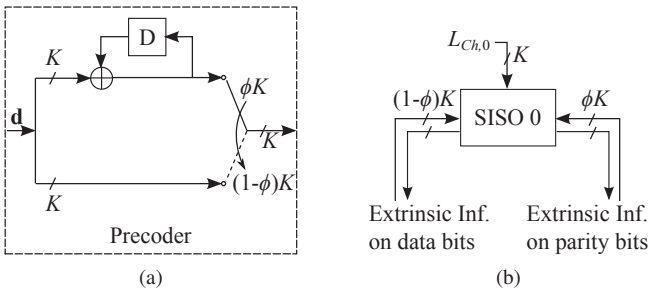

Fig. 6: (a) Hybrid precoding structure. (b) Extrinsic information exchanged by the SISO decoder of the accumulator.

The modified EXIT chart for different values of ϕ, evaluated over the AWGN channel, is shown in Fig. 7 and the corresponding error rate performance curves, obtained with uniform interleavers, are presented in Fig. 8. In Fig. 7, we can observe that the exchange of extrinsic information becomes less efficient when ϕ increases and when the SNR is kept constant. This is confirmed by Fig. 8. If low SNR region losses greater than 0.3 dB are not acceptable, values of ϕ higher than or equal to 0.1 should not be used.

According to the hybrid PTC error rate performance presented in Fig. 8, a good compromise between convergence and asymptotic performance for this block size and coding rate is obtained for ϕ equal to 0.04. For higher values of ϕ (e.g. $\phi = 0.1$), the improvement in error floor performance is not considered large enough to justify the resulting loss in convergence threshold. Note that, under the uniform interleaving assumption, the error floor gain obtained with the hybrid PTC with $\phi = 0.04$ is of almost one decade and a half, compared to the conventional TC.

B. Composite Precoding Structure

Trying to benefit from the convergence behavior and the error floor performance of the first and second previously introduced precoding structures, we combined the two of them in a new one and analyzed the resulting performance.

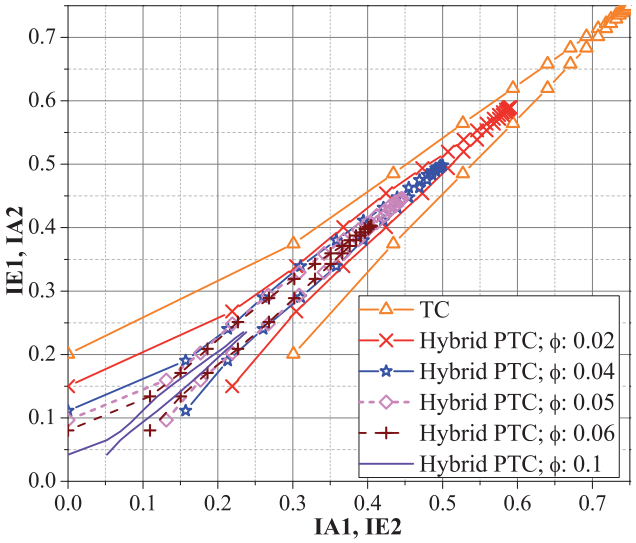

Fig. 7: Extrinsic information exchange between constituent codes of the TC at E_b/N_0 = 2.55 dB with 16 iterations of the hybrid PTC decoder for different values of ϕ, $K = 1504$, and $R = 4/5$ over the AWGN channel.

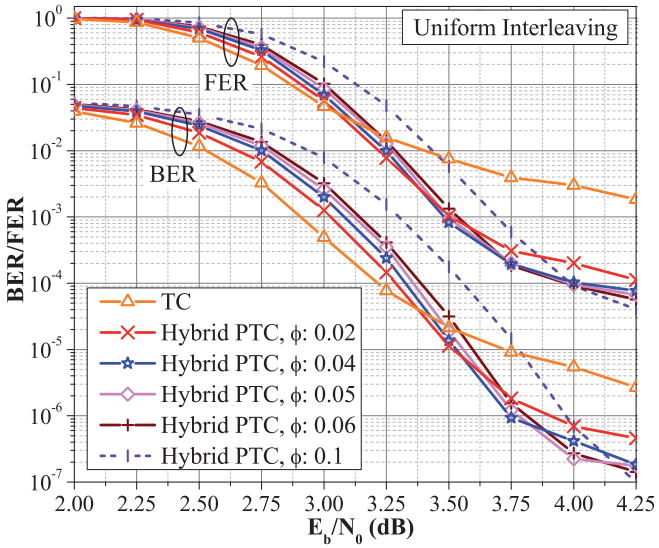

Fig. 8: Hybrid PTC error rate performance for different values of ϕ over the AWGN channel with BPSK modulation for $K = 1504$ and $R = 4/5$.

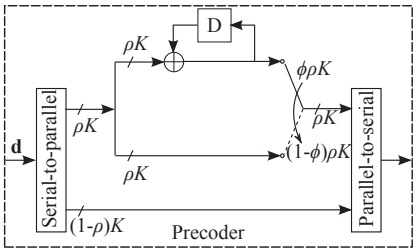

Fig. 9: Composite precoding structure.

The composite precoding structure has then two parameters ρ and ϕ (see Fig. 9), which represent the total and serial-to-parallel precoding ratios as in the original structures. In order to reduce the research complexity of an optimal couple of parameters ρ and ϕ, two strategies based on the extreme cases are adopted.

In the first strategy, for the same block size and coding rate as in in Section II, ρ is set to 0.11 and ϕ to 1. The resulting structure corresponds to the optimal configuration obtained for the original PTC ($\rho = 0.11$, see Fig. 5). Then, ϕ is decreased and the corresponding modified EXIT charts are plotted (see Fig. 10). When the value of ϕ decreases, the convergence performance of the composite PTC approaches the one of the classic TC. The composite PTC error rate performance, for the couples of ρ and ϕ considered in this strategy, is shown in Fig. 11. The convergence behavior of the code corresponds to the one predicted in the EXIT chart analysis. In addition, no improvement in error floor performance is obtained.

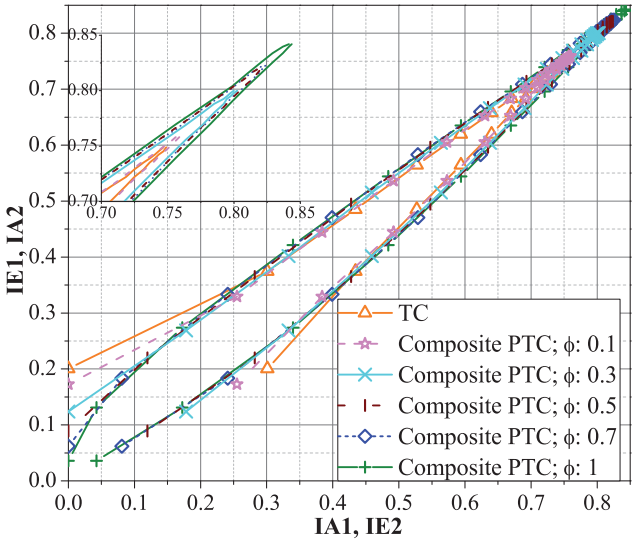

Fig. 10: Extrinsic information exchange between constituent codes of the TC at E_b/N_0 = 2.55 dB with 16 iterations of the composite PTC decoder for $\rho = 0.11$ and different values of ϕ, $K = 1504$, and $R = 4/5$ over the AWGN channel.

In the second strategy, ρ is set to 1 and ϕ to 0.04, which corresponds to its optimal value for the hybrid precoding structure proposed in Section III-A. Then, ρ is decreased and the corresponding modified EXIT charts are plotted (see Fig. 12). They show that the convergence threshold is expected to decrease when the value of ρ diminishes.

The corresponding error rate performance with uniform interleaving is shown in Fig. 13. It is in accordance with the EXIT chart analysis. Convergence improvements are achieved by decreasing the value of ρ at the expense of a loss in error floor performance, compared to the one obtained with the optimal configuration of the hybrid precoding structure ($\phi = 0.04$). Note that any convergence improvement will not enable the considered structure to surpass the case where $\rho = 0.11$ shown in Fig.5.

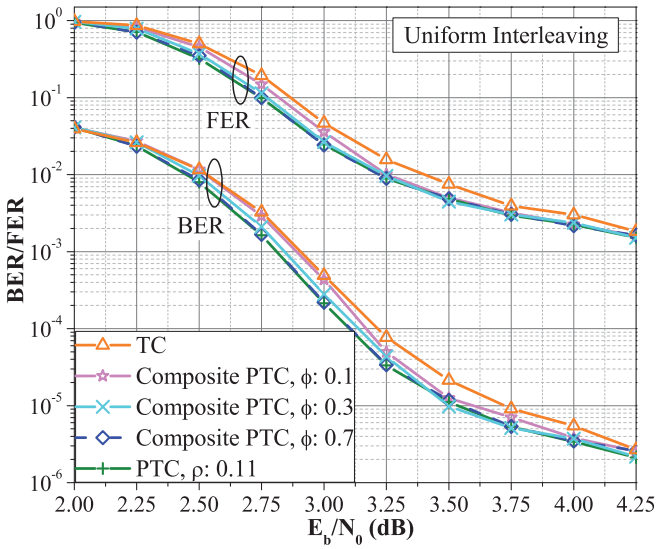

Fig. 11: Composite PTC error rate performance for $\rho = 0.11$ and different values of ϕ, over the AWGN channel with BPSK modulation for $K = 1504$ and $R = 4/5$.

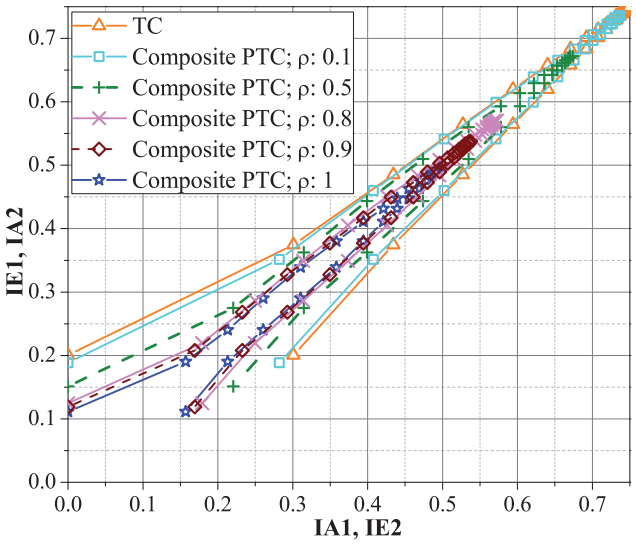

Fig. 12: Extrinsic information exchange between constituent codes of the TC at E_b/N_0 = 2.55 dB with 16 iterations of the composite PTC decoder for $\phi = 0.04$ and different values of ρ, $K = 1504$, and $R = 4/5$ over the AWGN channel.

C. Conclusion

Three different precoding structures were analyzed. It was shown that convergence improvements are achieved with the reference precoding structure introduced in [5] compared to a classic TC. Furthermore, a significant asymptotic gain is attained with the proposed hybrid precoding structure.

The combination of the first two precoding schemes was also studied. It was observed that the composite precoding structure shows a performance level that can be considered as a compromise between the original structure with improved

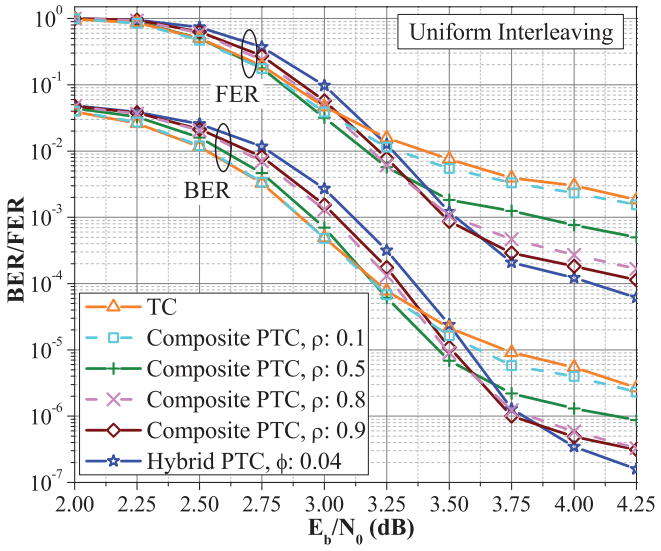

Fig. 13: Composite PTC error rate performance for $\phi = 0.04$ and different values of ρ, over the AWGN channel with BPSK modulation for $K = 1504$ and $R = 4/5$.

convergence threshold and the hybrid precoding structure with improved error floor. It could not solve the convergence versus error floor tradeoff issue. However, it remains of interest for communication systems requiring the adaptation of channel coding to the encountered noise level.

Finally, taking the improvement in the error floor as target, the hybrid precoding structure with $\phi = 0.04$ is selected for the analysis in the following section.

IV. Relevant Interleaver Design Criteria for PTCs

In the previous analyses of PTCs, we have only considered uniform interleavers, representative of the average asymptotic performance over all the possible interleavers. In this section, we focus on the design of interleavers for PTC structures.

The hybrid PTC can be seen as a three-dimensional TC, in which the first dimension corresponds to the precoder and the other two dimensions correspond to the constituent codes of the TC. Therefore, the precoder and TC interleavers, Π_1 and Π_2, have to be designed considering the three-dimensional nature of the hybrid PTC. Thus, interleaver design criteria, such as span [10], [11] and correlation girth [12], proposed for a classic TC have to be revisited for the three-dimensional case.

A. Span Properties

As mentioned in [13], good span properties in Π_1 and Π_2 do not guarantee good span properties in the three dimensions of the code. In fact, the minimum span values $S_{\min 1}$, $S_{\min 2}$, and $S_{\min 1,2}$ of the three permutations Π_1, Π_2, and $\Pi_{1,2}$ (the permutation composed of Π_1 and Π_2), have to be maximized to guarantee good span properties in the three dimensions of the code.

B. Proposed Correlation Graph

The sequence at the input of Π_1, $\mathbf{d_1}$, the interleaved sequence at the output of Π_1, $\mathbf{d_2}$, and the interleaved sequence at the output of Π_2, $\mathbf{d_3}$, are represented in Fig. 14(a), considering tail-biting termination [14]. The correlation girths of Π_1 and Π_2 are g_1 and g_2, respectively and $g_{1,2}$ represents the correlation girth of the permutation composed of both interleavers, $\Pi_{1,2}$. Under this representation, the correlation graph of each interleaver corresponds to a regular graph of degree 4. However, a unified correlation graph, considering the three-dimensional nature of the code, corresponds to a regular graph of degree 6, as shown in Fig. 14(b). Therefore, the lower correlation girth among g_1, g_2, and $g_{1,2}$ can only be considered as an upper bound on the effective correlation girth g_{eff} of the unified correlation graph in Fig 14(b). Actually, the unified correlation graph of degree 6 has a lower theoretical upper bound (obtained using the Moore bound [15]) on its correlation girth than the independent correlation graphs of Π_1, Π_2, and $\Pi_{1,2}$ of degree 4. Thus, in order to reduce the correlation among the exchanged extrinsic information by the precoder and the constituent codes of the TC, g_{eff} has to be maximized.

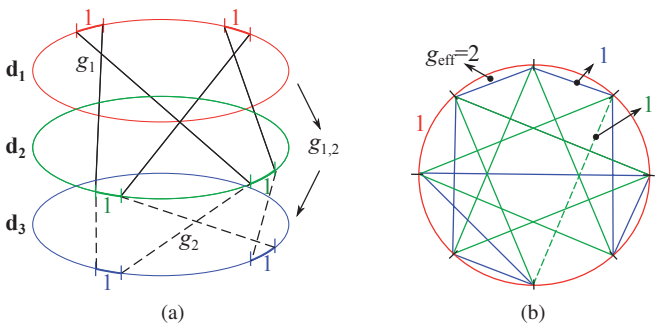

Fig. 14: Example of independent representation of the correlation graphs in the three dimensions of the code (a) and unified representation of the correlation graph (b) for Π_1, Π_2, and $\Pi_{1,2}$.

V. Example of Hybrid PTC with Optimized Interleavers

We have designed interleavers for the hybrid PTC scheme based on the Almost Regular Permutation (ARP) [11] model. As shown in [16], the ARP interleaver is a sufficient permutation model to design TCs with minimum Hamming distances *as high as* the most popular interleavers for TCs (i.e., DRP [17] and QPP [18]). Therefore, the ARP model is selected for the interleavers of the proposed hybrid PTC. This model considers circular constituent codes in the TC encoder.

Since the design of an efficient couple of interleavers Π_1 and Π_2 is more complex than the search for a single interleaver in the case of a conventional TC, we divided the selection process of Π_1 and Π_2 into the following steps.

1) *Generate ARP candidates for* Π_2: A group of ARP interleaver candidates for Π_2 is generated. The values

of $S_{\min 2}$ and g_2 are maximized by construction due to the ease of including these criteria in the ARP model.

2) *Select* Π_2 *in terms of the TC* $d_{\min}$: The best candidate for Π_2 is identified as the one providing the larger minimum Hamming distance $d_{\min}$ value in the TC.
3) *Identify the best ARP candidates for* Π_1: A group of interleaver candidates for Π_1 is generated as in step 1. Then, a restricted group of candidates for Π_1 is composed of the candidates allowing the larger values of $S_{\min 1,2}$ and $g_{1,2}$.
4) *Select* Π_1 *in terms of the hybrid PTC* $d_{\min}$: Finally, the best candidate for Π_1 is determined as the one generating the larger $d_{\min}$ value in the hybrid PTC.

These guidelines were applied to design interleavers for the hybrid PTC with coding rate $R=4/5$ and data sequence size $K = 1504$. Error rate performance was simulated over the AWGN channel with a BPSK modulation and a maximum of sixteen decoding iterations, using the Maximum *A Posteriori* (MAP) algorithm [19].

Fig. 15 shows the Frame Error Rate (FER) performance of the hybrid PTC using the selected couple of interleavers for Π_1 and Π_2, whose $d_{\min}$ is equal to 11. We observe that the error floor performance of a classic TC, using tail-biting termination and an ARP interleaver with $d_{\min}$ of 9, is improved by almost two decades with the proposed hybrid PTC. In addition, the proposed hybrid PTC achieves a gain of about 0.38 dB in convergence and almost 4 decades in error floor, compared to the puncturing pattern and the interleaver adopted in LTE.

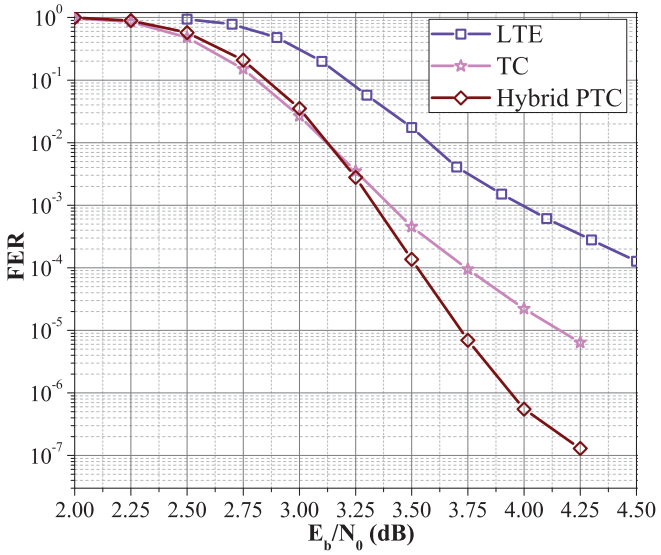

Fig. 15: Frame error rate performance comparison among the hybrid PTC for $\phi = 0.04$, a classic TC, and the LTE system over the AWGN channel for $R=4/5$, $K=1504$, and CRSC constituent codes with generator polynomials $(13, 15)_8$.

VI. Conclusion

This paper studies three different structures for PTCs. The conventional EXIT chart tool could not be exploited to predict PTC decoding convergence behaviour. Therefore, we proposed an analysis based on the *real exchange* of extrinsic information between the constituent SISO decoders, within actual PTC decoding iterations, to efficiently select the best precoder parameters in terms of convergence. We also introduced two new precoding structures and we presented design criteria leading to good interleavers for PTCs. We showed that significant asymptotic performance improvements can be achieved with the proposed hybrid PTC scheme.

References

[1] C. Berrou, A. Glavieux, and P. Thitimajshima, "Near shannon limit error-correcting coding and decoding: Turbo-codes," in *Proc. IEEE International Conference on Communications, (ICC'93)*, vol. 2, Geneva, Switzerland, May 1993, pp. 1064–1070.

[2] D. Divsalar, H. Jin, and R. McEliece, "Coding theorems for "turbo-like" codes," in *Proc. 36th Annual Allerton Conference on Comm., Control, and Computing*, Allerton, IL, USA, Sept. 1998, pp. 201–210.

[3] K. Gracie and M. Hamon, "Turbo and turbo-like codes: Principles and applications in telecommunications," *Proc. IEEE*, vol. 95, no. 6, pp. 1228–1254, June 2007.

[4] A. Abbasfar, D. Divsalar, and K. Yao, "Accumulate repeat accumulate codes," in *Proc. IEEE Global Telecommun. Conf.*, vol. 1, Dallas, Texas, USA, Nov 2004, pp. 509–513.

[5] S. Tong, H. Zheng, and B. Bai, "Precoded turbo code within 0.1 dB of Shannon limit," *Electron. Lett.*, vol. 47, no. 8, pp. 521–522, April 2011.

[6] ETSI, "LTE Envolved Universal Terrestrial Radio Access(E-UTRA): Multiplexing and channel coding," TS 136 212 (V10.0.0), January 2011.

[7] S. ten Brink, "Convergence behavior of iteratively decoded parallel concatenated codes," *IEEE Trans. Commun.*, vol. 49, no. 10, pp. 1727–1737, Oct. 2001.

[8] J. Hagenauer, "The EXIT chart - Introduction to extrinsic information transfer in iterative processing," in *Proc. 12th Europ. Signal Proc. Conf (EUSIPCO)*, Sept. 2004, pp. 1541–1548.

[9] S. Benedetto and G. Montorsi, "Unveiling turbo codes: some results on parallel concatenated coding schemes," *IEEE Trans. Inf. Theory*, vol. 42, no. 2, pp. 409–428, 1996.

[10] S. Crozier, "New high-spread high-distance interleavers for turbo-codes," in *Proc. 20th Biennial Symposium on Communications, Queen's University*, Kingston, Ontario, Canada, May 2000, pp. 3–7.

[11] C. Berrou, Y. Saouter, C. Douillard, S. Kerouedan, and M. Jezequel, "Designing good permutations for turbo codes: towards a single model," in *Proc. IEEE International Conference on Communications, (ICC'04)*, vol. 1, Paris, France, Jun. 2004, pp. 341–345.

[12] Y. Saouter, "Selection procedure of turbocode parameters by combinatorial optimization," in *Proc. 6th Int. Symposium on Turbo Codes and Iterative Information Processing (ISTC)*, Brest, France, Sept. 2010, pp. 156–160.

[13] D. Gnaedig, E. Boutillon, and M. Jézéquel, "Design of three-dimensional multiple slice turbo codes." *EURASIP J. Adv. Sig. Proc.*, vol. 2005, no. 6, pp. 808–819, May 2005.

[14] C. Weiss, C. Bettstetter, and S. Riedel, "Code construction and decoding of parallel concatenated tail-biting codes," *IEEE Trans. Inf. Theory*, vol. 47, no. 1, pp. 366–386, Jan 2001.

[15] N. Biggs, "Minimal regular graphs with given girth," in *Algebraic graph theory*. New York, NY, USA: Cambridge University Press, 1974, pp. 180–190.

[16] R. Garzón Bohórquez, C. Abdel Nour, and C. Douillard, "On the equivalence of interleavers for turbo codes," *IEEE Wireless Commun. Lett.*, vol. 4, no. 1, pp. 58–61, Feb. 2015.

[17] S. Crozier and P. Guinand, "High-performance low-memory interleaver banks for turbo-codes," in *Proc. IEEE 54th Vehicular Technology Conference (VTC 2001-Fall)*, vol. 4, Atlantic City, NJ, USA, Oct. 2001, pp. 2394–2398.

[18] J. Sun and O. Takeshita, "Interleavers for turbo codes using permutation polynomials over integer rings," *IEEE Trans. Inf. Theory*, vol. 51, no. 1, pp. 101–119, Jan. 2005.

[19] L. Bahl, J. Cocke, F. Jelinek, and J. Raviv, "Optimal decoding of linear codes for minimizing symbol error rate (corresp.)," *IEEE Trans. Inf. Theory*, vol. 20, no. 2, pp. 284–287, Mar 1974.